Journal of Reinforced Plastics and Composites
http://jrp.sagepub.com

Pseudo-Transient Analysis of Composite Shells Including Geometric and Material Non-Linearities

J.R. Kommineni and T. Kant

Journal of Reinforced Plastics and Composites 1993; 12; 101
DOI: 10.1177/073168449301200106

The online version of this article can be found at:
http://jrp.sagepub.com/cgi/content/abstract/12/1/101

Published by:
SAGE Publications
http://www.sagepublications.com

Pseudo-Transient Analysis of Composite Shells Including Geometric and Material Non-Linearities

J. R. KOMMINENI* AND T. KANT**
Department of Civil Engineering
Indian Institute of Technology
Powai, Bombay 400–076
India

ABSTRACT: An unified approach is presented for the pseudo-transient (static) linear, geometric, material and combined geometric and material non-linear analyses of laminated composite shells. A nine-noded isoparametric quadrilateral finite element belonging to the Lagrangian family is used in space discretization. An explicit time marching scheme is employed for time integration of the resulting discrete ordinary differential equations with the special forms of diagonal fictitious mass and/or damping matrices. The elasto-plastic material behaviour is incorporated using a flow theory of plasticity. In particular, the modified version of Hill's initial yield criterion is used in which anisotropy parameters of plasticity are introduced. The shear deformation is accounted for using an extension of Sander's shell theory, and the geometric non-linearity is considered in the sense of von Karman strains. The layered element approach is adopted for the treatment of elasto-plastic behaviour through the thickness. A wide range of numerical examples are presented to demonstrate the validity and efficiency of the present approach. The results for combined non-linearity are also presented. The variety of results presented here is based on realistic material properties of more commonly used advanced composite materials. The results of the combined non-linear analysis should serve as reference for future investigations.

1. INTRODUCTION

IN RECENT YEARS composites, especially fibre reinforced laminated plates and shells, have found increasing application in many engineering structures. This is mainly due to two desirable features of fibre reinforced composites, viz., the high stiffness to weight ratio, and the anisotropic material property that can be tailored through the variation of the fibre orientation and stacking sequence of laminas, a feature that gives the designer an added degree of flexibility. Because of the high modulus and high strength properties that composites have, structural

*Research Scholar.
**Professor.

0731-6844/93/01 0101-26 $6.00/0

composites undergo large deformations in elastic and inelastic ranges. Therefore, an accurate response prediction is possible only when one considers the geometric and material non-linearities. In this article, an unified approach for the static, linear, and geometric non-linear, elastic and elasto-perfectly plastic analyses of laminated composite shells is presented.

The origin of this approach dates back to 1965, when the method of dynamic relaxation was introduced by Day [1]. Since then, many research workers have contributed to the development of this method by applying it to a variety of problems [2–5]. This method is essentially a step-by-step integration of critically damped vibration using fictitious mass and/or viscous damping to ensure the attainment of a steady-state solution as fast as possible. Even though the use of the finite difference in space method compares well with the finite element method, the difficulties encountered with complicated geometries make its use unattractive. Thus, maintaining the generality of the finite element method and the wide spectrum of software available thereon, it is advisable to develop the relaxation procedure with respect to space discretization by finite elements. Pica and Hinton [6–7] used this approach for linear and geometrically non-linear analyses of isotropic Mindlin plates. Kant and Patel [8] extended this approach to two-dimensional small and large deformation elastic problems (plane stress/plane strain and axisymmetric). To the authors' knowledge, there exist no results in open literature on non-linear pseudo-transient analysis of composite shells. The present investigation tries to fill this gap and is concerned with the pseudo-transient (static) analysis of layered composite shells under the applied transverse loads that includes both geometric and material non-linearities.

2. THEORY

The laminated shell considered here is composed of a finite number of orthotropic layers, with principal material axes of elasticity oriented arbitrarily with respect to the shell axes. The x, y coordinates of the shell are taken at the mid-surface of the shell (see Figure 1), and the displacement model is assumed to be of the form,

$$\begin{aligned} u(x,y,z,t) &= u_o(x,y,t) + z\theta_x(x,y,t) \\ v(x,y,z,t) &= v_o(x,y,t) + z\theta_y(x,y,t) \\ w(x,y,z,t) &= w_o(x,y,t) \end{aligned} \tag{1}$$

where the subscript "o" denotes mid-surface values, and θ_x and θ_y are the rotations of the mid-surface normals in the xz and yz surfaces, respectively. In the present investigation, large displacements are considered in the sense of von Karman, which implies that the first derivatives of tangential displacement components with respect to x, y, and z are small so that their particular products can be neglected (see e.g., Reddy and Chandrashekhara [9]). The elasto-perfectly plastic analysis is based on Huber-Mises yield criterion extended by Hill for aniso-

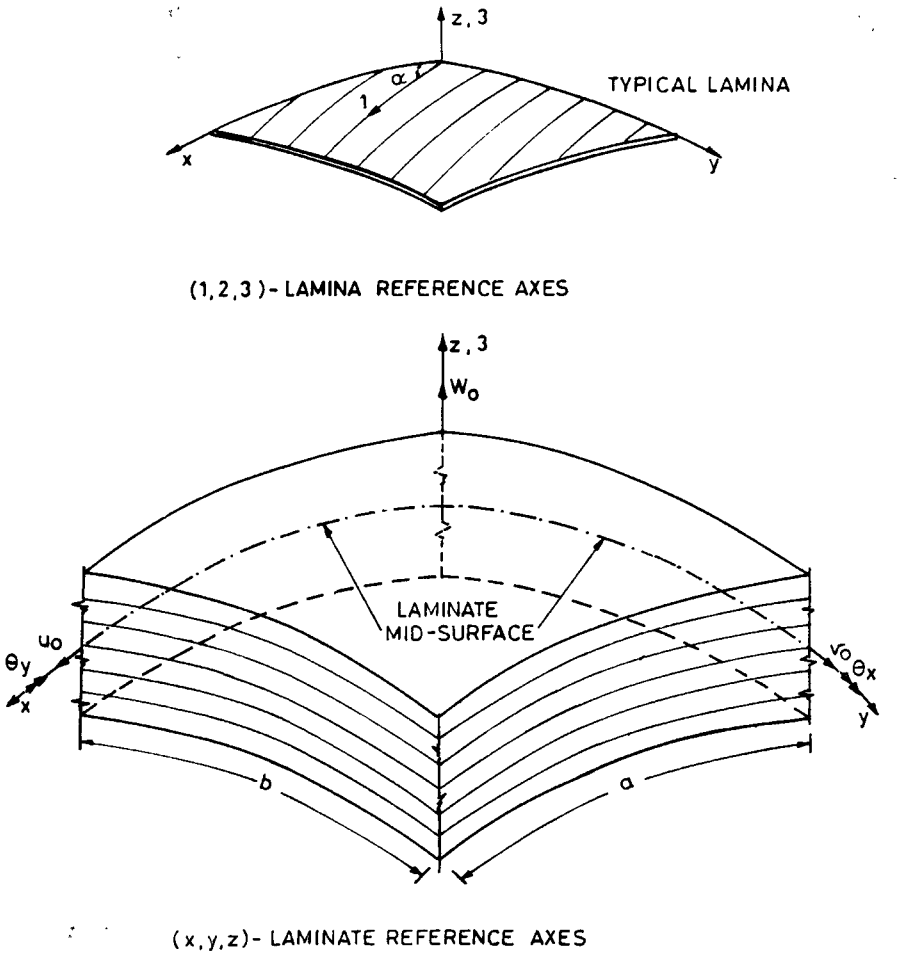

Figure 1. *Laminate geometry with positive set of lamina/laminate reference axes, displacement components and fibre orientation.*

tropic materials. The yield function is generalized by introducing anisotropic parameters of plasticity.

The strain expressions are derived by modifying the Sanders' shell theory [10] by including the first order shear deformation effects. The incremental strains can be written as follows,

$$\delta\epsilon_x = \delta\epsilon_{xo} + z\delta\varkappa_x;\ \delta\epsilon_y = \delta\epsilon_{yo} + z\delta\varkappa_y;$$

$$\delta\gamma_{xy} = \delta\epsilon_{xyo} + z\delta\varkappa_{xy};\ \delta\gamma_{xz} = \delta\phi_x;\ \delta\gamma_{yz} = \delta\phi_y \qquad (2a)$$

in which

$$[\delta\epsilon_{xo}, \delta\epsilon_{yo}\delta\epsilon_{xyo}] = \left[\frac{\partial\delta u_o}{\partial x} + \frac{\delta w_o}{R_1} + \frac{\partial w_o}{\partial x}\frac{\partial\delta w_o}{\partial x};\right.$$
$$\frac{\partial\delta v_o}{\partial y} + \frac{\delta w_o}{R_2} + \frac{\partial w_o}{\partial y}\frac{\partial\delta w_o}{\partial y};$$
$$\left.\frac{\partial\delta v_o}{\partial x} + \frac{\partial\delta u_o}{\partial y} + \frac{\partial w_o}{\partial x}\frac{\partial\delta w_o}{\partial y} + \frac{\partial\delta w_o}{\partial x}\frac{\partial w_o}{\partial y}\right] \tag{2b}$$
$$[\delta\kappa_x, \delta\kappa_y, \delta\kappa_{xy}] = \left[\frac{\partial\delta\theta_x}{\partial x}; \frac{\partial\delta\theta_y}{\partial y}; \frac{\partial\delta\theta_y}{\partial x} + \frac{\partial\delta\theta_x}{\partial y}\right.$$
$$\left. + \frac{1}{2}\left(\frac{1}{R_2} - \frac{1}{R_1}\right)\left(\frac{\partial\delta v_o}{\partial x} - \frac{\partial\delta u_o}{\partial y}\right)\right]$$
$$[\delta\phi_x, \delta\phi_y] = \left[\delta\theta_x + \frac{\partial\delta w_o}{\partial x} - \frac{\delta u_o}{R_1}; \delta\theta_y + \frac{\partial\delta w_o}{\partial y} - \frac{\delta v_o}{R_2}\right]$$

The elastic stress-strain relations for a typical layer L with reference to the material axes (1,2,3) are given by

$$\begin{bmatrix}\sigma_1\\ \sigma_2\\ \tau_{12}\\ \tau_{13}\\ \tau_{23}\end{bmatrix}^L = \begin{bmatrix}C_{11} & C_{12} & 0 & 0 & 0\\ C_{12} & C_{22} & 0 & 0 & 0\\ 0 & 0 & C_{33} & 0 & 0\\ 0 & 0 & 0 & \beta C_{44} & 0\\ 0 & 0 & 0 & 0 & \beta C_{55}\end{bmatrix}^L \begin{bmatrix}\epsilon_1\\ \epsilon_2\\ \gamma_{12}\\ \gamma_{13}\\ \gamma_{23}\end{bmatrix}^L \tag{3}$$

in which $[\sigma_1, \sigma_2, \tau_{12}, \tau_{13}, \tau_{23}]$ are the elastic-stresses and $[\epsilon_1, \epsilon_2, \gamma_{12}, \gamma_{13}, \gamma_{23}]$ are the physical strain components referred to the material or lamina axes (1,2,3) as shown in Figure 1. C_{ij}s are the composite material stiffness coefficients of the L^{th} lamina in the lamina axes (1,2,3), and β is the usual shear correction coefficient and is assumed here to take the usual value of 5/6.

Following the usual transformation rules of stresses/strains between the layer and laminate coordinate systems, the stress-strain relations for the L^{th} layer in the laminate coordinates (x,y,z) are written in a compact form (see Kant and Kommineni [11]) as:

$$\delta\boldsymbol{\sigma} = \mathbf{Q}\,\delta\boldsymbol{\epsilon} \tag{4a}$$

in which $\delta\boldsymbol{\sigma} = (\delta\sigma_x, \delta\sigma_y, \delta\tau_{xy}, \delta\tau_{xz}, \delta\tau_{yz})^t$ is the elastic incremental stress vector and $\delta\boldsymbol{\epsilon} = (\delta\epsilon_x, \delta\epsilon_y, \delta\gamma_{xy}, \delta\gamma_{xz}, \delta\gamma_{yz})^t$ is the incremental strain vector with respect to shell axes. The superscript "t" indicates the transposition of a matrix/

vector and the non-zero elements of **Q** matrix which is of size 5 × 5, and are defined as follows,

$$Q_{11} = C_{11} \cdot c^4 + (2 \cdot C_{12} + 4 \cdot C_{33}) \cdot s^2 \cdot c^2 + C_{22} \cdot s^4$$

$$Q_{12} = C_{12} \cdot (c^4 + s^4) + (C_{11} + C_{22} - 4 \cdot C_{33}) \cdot s^2 \cdot c^2$$

$$Q_{13} = (C_{11} - C_{12} - 2 \cdot C_{33}) \cdot s \cdot c^3 + (C_{12} - C_{22} + 2 \cdot C_{33}) \cdot s^3 \cdot c$$

$$Q_{22} = C_{11} \cdot s^4 + (2 \cdot C_{12} + 4 \cdot C_{33}) \cdot s^2 \cdot c^2 + C_{22} \cdot c^4$$

$$Q_{23} = (C_{11} - C_{12} - 2 \cdot C_{33}) \cdot s^3 \cdot c + (C_{12} - C_{22} + 2 \cdot C_{33}) \cdot s \cdot c^3 \quad (4b)$$

$$Q_{33} = C_{33} \cdot (c^4 + s^4) + (C_{11} - 2 \cdot C_{12} + C_{22} - 2 \cdot C_{33}) \cdot s^2 \cdot c^2$$

$$Q_{44} = C_{44} \cdot c^2 + C_{55} \cdot s^2$$

$$Q_{45} = C_{44} - C_{55}) \cdot c \cdot s$$

$$Q_{55} = C_{44} \cdot s^2 + C_{55} \cdot c^2$$

where $c = \cos\theta$ and $s = \sin\theta$.

The laminate constitutive relations involving membrane forces, bending moments, and shear forces are defined as:

$$\begin{bmatrix} N_x, N_y, N_{xy} \\ M_x, M_y, M_{xy} \\ Q_x, Q_y \end{bmatrix} = \sum_{L=1}^{NL} \begin{bmatrix} \sigma_x \ \sigma_y \ \tau_{xy} \\ \bar{z}\sigma_x \ \bar{z}\sigma_y \ \bar{z}\tau_{xy} \\ \tau_{xz} \ \tau_{yz} \end{bmatrix} h_L \quad (5)$$

where

$$H_L = z_{L+1} - z_L \text{ and } \bar{z} = \left(\frac{z_{L+1} + z_L}{2}\right)$$

3. FINITE ELEMENT FORMULATION

The finite element used here is a nine-noded quadrilateral element of the Lagrangian family. The laminate displacement field in the element can be expressed in terms of nodal variables as:

$$\mathbf{d}(\epsilon,\eta) = \sum_{i=1}^{NN} N_i(\xi,\eta) \cdot \mathbf{d}_i \quad (6)$$

where NN is number of nodes per element, $N_i(\xi,\eta)$ contains interpolation functions associated with node i in terms of local coordinates ξ, η, and $\mathbf{d}_i$ is nodal dis-

placement vector such that $\mathbf{d}_i^t = (u_{oi}, v_{oi}, w_{oi}, \theta_{xi}, \theta_{yi})$. The strain displacement relations can be written as follows (see Zienkiewicz [13]):

$$\bar{\epsilon} = \left(\mathbf{B}_o + \frac{1}{2}\mathbf{B}_{NL}\right) \cdot \mathbf{a} \tag{7a}$$

$$\delta\bar{\epsilon} = (\mathbf{B}_o + \mathbf{B}_{NL}) \cdot \delta\mathbf{a} \tag{7b}$$

also

$$\delta\bar{\epsilon} = \sum_{i=1}^{NN} \mathbf{B}_i \cdot \delta\mathbf{d}_i = \mathbf{B}\,\delta\mathbf{a} \tag{7c}$$

where $\mathbf{B}_o$ is the strain matrix giving linear strains, $\mathbf{B}_{NL}$ is linearly dependent upon the nodal displacement vector $\mathbf{a}$, such that $\mathbf{a}^t = (\mathbf{d}_1^t, \mathbf{d}_2^t, \ldots, \mathbf{d}_{NN}^t)$. The non-zero coefficients of the $\mathbf{B}_i$ sub-matrix of size 8×5 are defined as follows:

$$B_{11} = B_{32} = B_{43} = B_{64} = B_{85} = \frac{\partial N_i}{\partial x}$$

$$B_{44} = B_{55} = N_i$$

$$B_{22} = B_{31} = B_{53} = B_{75} = B_{84} = \frac{\partial N_i}{\partial y}$$

$$B_{13} = \frac{N_i}{R_1} + \frac{\partial w_o}{\partial x} \cdot \frac{\partial N_i}{\partial x}$$

$$B_{23} = \frac{N_i}{R_2} + \frac{\partial w_o}{\partial y} \cdot \frac{\partial N_i}{\partial y}$$

$$B_{33} = \frac{\partial w_o}{\partial x} \cdot \frac{\partial N_i}{\partial y} + \frac{\partial w_o}{\partial y} \frac{\partial N_i}{\partial x}$$

$$B_{81} = \frac{1}{2}\left(\frac{1}{R_1} - \frac{1}{R_2}\right) \cdot \frac{\partial N_i}{\partial y}$$

$$B_{82} = \frac{1}{2}\left(\frac{1}{R_2} - \frac{1}{R_1}\right) \cdot \frac{\partial N_i}{\partial x}$$

$$B_{41} = -\frac{N_i}{R_1}$$

$$B_{52} = -\frac{N_i}{R_2} \tag{8}$$

3.1 Layered Model Approach

The concept of the layered model approach is introduced in order to handle the plasticity in the cross section of the element in which progressive yielding through thickness of laminate is accounted for by depicting it as a collection of thin layers (Owen and Hinton [12]). Accurate representation of the stress is particularly important in the plasticity analysis with variation of properties from layer to layer accounted.

3.2 Plastic Correction

For the yielded Gauss points, the stresses are calculated so that the yielding criterion is satisfied. If the actual stress is found greater than this permissible value, then the portion of the stress greater than the yield value must be reduced to the yield surface. Consider the situation for the r^{th} iteration of any particular load increment (see Figure 2a). On loading from point C, the stress point moves elastically until yield surface is met at B. Elastic behaviour beyond this point will result in a final stress state defined by point A. However, in order to satisfy the yielding criterion, the stress point cannot move outside the yield surface and thus can only traverse the surface until the yield criterion (see Appendix A) and constitutive relations are satisfied.

To reduce the stress to the yield surface for the yielded Gauss points, the following steps are considered.

STEP A

Compute the incremental changes, $d\sigma_e^r$, where subscript "e" denotes that we are assuming elastic behaviour.

STEP B

Accumulate the total stress for each element Gauss point as

$$\sigma_e^r = \sigma_e^{r-1} + d\sigma_e^r \tag{9a}$$

STEP C

Calculate the effective stresses $\bar{\sigma}_e^{r-1}$ and $\bar{\sigma}_e^r$ and check for the following cases:

Case 1

$$\bar{\sigma}_e^{r-1} < \sigma_y \text{ and } \bar{\sigma}_e^r < \sigma_y$$

Elastic point is still elastic. No reduction of stress is required.

Case 2

$$\bar{\sigma}_e^{r-1} > \sigma_y \text{ and } \bar{\sigma}_e^r < \sigma_y$$

Elastic point now unloading. No reduction of stress is required.

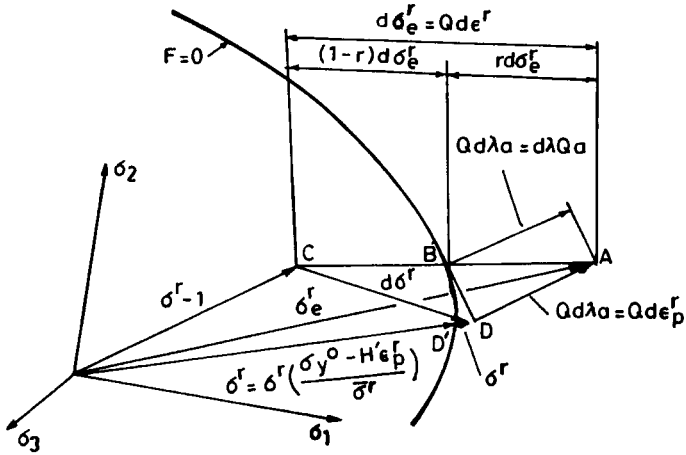

Figure 2a. *Incremental stress changes at a point in an elasto-plastic continuum at initial yield (taken from Owen and Hinton [12]).*

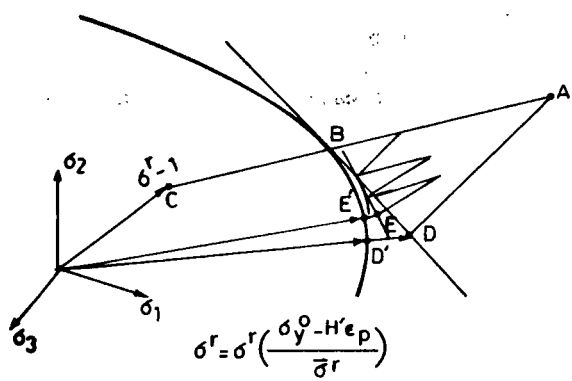

Figure 2b. *Refined process for reducing a stress point to the yield surface (taken from Owen and Hinton [12]).*

Case 3

$$\bar{\sigma}_e^{r-1} < \sigma_y \text{ and } \bar{\sigma}_e^{r} > \sigma_y$$

Elastic point becomes plastic. The portion of the stress greater than the yield value must be reduced to the yield surface.

Case 4

$$\bar{\sigma}_e^{r-1} > \sigma_y \text{ and } \bar{\sigma}_e^{r} > \sigma_y$$

Plastic point goes further plastic. Reduce the entire increase in stress to remain on the yield surface.

STEP D

For the yielded Gauss points only, namely for cases (3) and (4), compute the portion of the total stress which satisfies the yielding criterion as

$$\sigma_e^r = \sigma_e^{r-1} + (1 - \xi)\, d\sigma_e^r \tag{9b}$$

where $\xi = (\bar{\sigma}_e^{r} - \sigma_y)/(\bar{\sigma}_e^{r} - \bar{\sigma}^{r-1})$ for case (3), and $\xi = 1$ for case (4).

STEP E

The remaining portion of stress, $\xi\, d\sigma_e^r$, must be effectively eliminated in some way. Point A must be brought onto the yield surface by allowing plastic deformation to occur. Physically this can be described as follows. On loading from point C, the stress point moves elastically until the yield surface is met at B. Elastic behaviour beyond this point would result in a final stress state defined by point A. However, in order to satisfy the yield criterion, the stress point cannot move outside the yield surface and consequently, the stress point can only traverse the surface until both equilibrium conditions and constitutive relations are satisfied. In the case of elasto-plastics, the incremental stress can be expressed as (see Owen and Hinton [12]):

$$d\sigma^r = Q d\epsilon^r - d\lambda d_{\mathrm{D}} \tag{9c}$$

$$\sigma^r = \sigma^{r-1} + d\sigma_e^r - d\lambda d_{\mathrm{D}} \tag{9d}$$

which gives the total stress σ^r satisfying the elasto-plastic conditions when the stresses are incremented from σ^{r-1}. It is evident that if a finite sized stress increment is taken, the final stress point D, corresponding to σ^r, may depart from the yield surface. This discrepancy can be eliminated by ensuring that the load increments considered in solution are sufficiently small. However, point D can be brought onto the yield surface by simply scaling the vector σ^r, denoting the effective stress due to stress σ^r as $\sigma^{r|}$, and noting that this value should coincide with

$\sigma_y = \sigma_y^o + H' \epsilon_p^{r'}$. If the point D lies on the yield surface, the appropriate scaling factor is readily seen to be

$$\sigma^r = \sigma^r \left(\frac{\sigma_y^o + H' \epsilon_p^{r'}}{\sigma^{r'}} \right) \tag{10}$$

This represents a scaling of the stress vector σ^r, which implies that the individual stress components are proportionally reduced. The normality condition for the plastic strain increment is evident from

$$\mathbf{Q} d\lambda \mathbf{a} = \mathbf{Q} d\epsilon_p \tag{11}$$

If relatively large load increment sizes are to be permitted, the process described above can lead to an inaccurate prediction of the final point D on the yield surface if the stress point is in the vicinity of a region of large curvature of the yield surface. This is illustrated in Figure 2b, where the process of reducing the elastic stress to the yield surface is shown to end in the stress point D, which is then scaled down to the yield surface to give point D, which is then further scaled down to the yield surface to give point D'. Greater accuracy can be achieved by relaxing the excess stress to the yield surface in several stages. Figure 2b shows the case where excess stress is divided into three equal parts and each increment reduced to yield surface in turn. After the reduction cycles, the stress point drifting away from the yield surface can be corrected by simply scaling to give final point E'. It is seen that the final points D' and E' can be significantly different. An additional refinement which can be introduced is to scale the stress point to the yield surface after the reduction process for each cycle, not only after the final cycle. Obviously, for the greater number of steps into which excess stress AB is divided, the greater will be the accuracy. However, the computation for each step is expensive since the vector $\mathbf{a}$ and $\mathbf{d}_D$ have to be calculated (see Appendix A) at each stage. Clearly, a balance must be sought and in this article, the following criterion is adopted. The excess stress $\xi d\sigma^r$ is divided into "m" parts, where m is given by the nearest integer value which is less than

$$\left(\frac{\sigma_e^{r'} - \sigma_y}{\sigma_y^o} \right) 8 + 1 \tag{12}$$

where $\sigma_e^{r'} - \sigma_y$ gives a measure of the excess stress AB, and σ_y^o is the initial yield stress.

However, for the elastic Gauss points, the stress σ^r is as follows

$$\sigma^r = \sigma^{r-1} + d\sigma_e^r \tag{13}$$

The discrete static equilibrium equations can be written as

$$\mathbf{P}(a,t) = \mathbf{f} \tag{14a}$$

and the discrete dynamic equations of motion as

$$\mathbf{P}(a,t) + \mathbf{C}\dot{\mathbf{a}} + \mathbf{M}\ddot{\mathbf{a}} = \mathbf{f} \tag{14b}$$

The reader is urged to refer to standard tests [13,14]. The static problem represented by the discrete Equation (14a) can be solved in a variety of ways. This generally requires a direct or factorized solution of simultaneous equations. An alternate solution procedure includes the transformation of Equation (14a) into dynamic equations of motion represented by Equation (14b) by inclusion of fictitious mass and/or damping matrices, and carrying out the dynamic analysis until a steady state is reached. In the above equation, **M** is the mass matrix, **C** is the damping matrix, $\mathbf{P}(a,t)$ is the vector of internal resisting forces, **f** is the vector of applied forces, **a** is the vector of nodal displacements, and a dot denotes differentiation with respect to the time.

(a) Internal force vector **P**:

$$\mathbf{P}(a,t) = \int_A \mathbf{B}^t \bar{\sigma} dA \tag{15}$$

where $\bar{\sigma}$ is stress-resultant vector.

(b) Mass matrix **M**: in the pseudo-transient analysis, the real mass is very seldom used. On the contrary, various forms of fictitious mass are introduced in order to increase the convergence rate towards the static equilibrium solution. Some commonly used forms in the literature are the following:

- a unit mass [15]
- a real mass matrix computed from different densities in u, v and w directions [16]
- a diagonal mass matrix obtained from the stiffness matrix **K** [4], in which the element $m_{ii} = \Sigma_{j=1}^{r} \mid K_{ij} \mid$, where r is the order of **K**
- a diagonal mass matrix obtained from the stiffness matrix **K** [4], in which the element $m_{ii} = K_{ii}$

It is noted from the available literature [6,7] that the last alternative produces the fastest convergence. Therefore, in the present investigation the diagonal terms of the linear stiffness matrix are taken as diagonal coefficients of diagonal fictitious mass matrix.

(c) Damping matrix **C**: the damping matrix is taken here as

$$\mathbf{C} = \alpha_c \mathbf{M} \tag{16a}$$

where α_c is the critical damping factor, such that $\alpha_c = 2\omega$ in which ω is the dominant frequency of the system. An eigenvalue analysis of the system for evaluating ω is generally avoided. In fact, it would be rather expensive and contrary to the main philosophy of pseudo-transient methods in which the aims are easy implementation and small computer core storage. In the present context, the

damping effect is included by considering the adaptive damping [7]. The critical damping factor α_c is given by,

$$\alpha_c = 2 \cdot \omega \tag{16b}$$

Here, the damping factor is constantly updated on the basis of the information gained during the current time step. It is thus possible to follow the behaviour of the structure during the integration in time very closely. It consists of using the Raleigh's quotient

$$\lambda_n = \left[\frac{\mathbf{a}_n^t \mathbf{K} \mathbf{a}_n}{\mathbf{a}_n^t \mathbf{M} \mathbf{a}_n}\right]^{1/2} \tag{17}$$

to estimate the lowest eigenvalue of the structure at the current time step. It is worth adding that the predicted value of α_c had to be scaled for maximum efficiency by a correction factor c_f.

Since the mass matrix **M** and damping matrix **C** are diagonal matrices, the set of Equation (14b) are uncoupled to give new displacement values without requiring the matrix factorization or any sophisticated solution techniques. The Equation (14b) can be written in a scalar form as:

$$m_i \ddot{a}_i + c_i \dot{a}_i + p_i = f_i \tag{18}$$

where subscript "i" denotes the i^{th} degree of freedom and the other symbols have the usual meanings.

In the explicit time marching scheme used here, the velocities and accelerations are approximated using the central difference formulae as:

$$\dot{a}_i^n = (a_i^{n+1} - a_i^{n-1})/2 \cdot \Delta t \tag{19a}$$

$$\ddot{\mathbf{a}}_i^n = (a_i^{n+1} - 2 \cdot a_i^n + a_i^{n-1})/\Delta t^2 \tag{19b}$$

where $n - 1$, n, and $n + 1$ denote three successive time stations. Using the above approximation, Equation (18) can be rewritten as:

$$m_i \cdot (a_i^{n+1} - 2 \cdot a_i^n + a_i^{n-1})/\Delta t^2 + c_i \cdot (a_i^{n+1} - a_i^{n-1})/2\Delta t + p_i^n - f_i^n = 0 \tag{20}$$

It becomes clear that the values of a_i^{n+1} can be determined from the two previous displacements, a_i^n and a_i^{n-1}, by rewriting Equation (20):

$$a_i^{n+1} = \left(m_i + c_i \frac{\Delta t}{2}\right)^{-1} \left[\Delta t^2 (f_i^n - p_i^n) + 2m_i \cdot a_i^n - \left(m_i - c_i \frac{\Delta t}{2}\right) \cdot a_i^{n-1}\right] \tag{21a}$$

If the values a^o and $\dot{a}^o$ are specified as initial conditions, a special starting algorithm can be written by noting that,

$$\dot{a}_i^o = (a_i^1 - a_i^{-1})/2 \cdot \Delta t \tag{21b}$$

and a_i^{-1} can be eliminated from Equation (21a).

The algorithm defined by Equations (21a and 21b) is very simple and easy to implement, but as is well-known, it is conditionally stable. This means that the time step length Δt must not exceed a given critical value for the scheme to be stable.

As a rough initial estimate, Δt for thin laminates of $a/h = 100$ is 1.2, and that for moderately thick laminates of $a/h = 10$ is 0.75, with correction factor $c_f = 0.75$ in the latter case, regardless of the size of the element used. However, the final value is based on economy and stability criteria.

4. SOLUTION TECHNIQUE

The essential steps in the computer code are as follows:

1. Read the input data.
2. Form the diagonal mass matrix **M** and external force vector **f**.
3. Apply the boundary conditions.
4. Evaluate the residual force vector $\mathbf{f}^n - \mathbf{p}^n$, however, in the first step, internal force vector **P** is taken to be zero.
5. Compute $\mathbf{a}^{n+1}$ from the $\mathbf{a}^n$ and $\mathbf{a}^{n-1}$.
6. Evaluate the new internal force vector $\mathbf{p}^{n+1}$ from $\mathbf{a}^{n+1}$.
7. Output the required values.
8. Introduce the time stepping procedure.

The following operations are carried out as explained below when damping effect is included by considering adaptive damping.

- The critical damping factor is determined in each step by using Equation (17). It is worth noting that the technique does not involve much additional computational efforts, in that $\mathbf{K}(a)\,\mathbf{a}^n = \mathbf{p}^n$ is already available, and **M** is a diagonal matrix.

The typical time history of a generalized displacement during the pseudo-transient analysis by including damping effects by means of adaptive damping can be seen in Figure 6.

- The convergence to static solution is checked, i.e., by using the convergence check either in terms of residual forces, or in terms of displacements. Steps 4 to 8 are performed until the system reaches a steady-state.

The convergence factors R and D, with respect to the residual forces and displacements, respectively, are defined as follows (see Pica and Hinton [6,7]):

$$R = \frac{\sqrt{\sum_{i=1}^{NV}(f_i - p_i)^2}}{\sqrt{\sum_{i=1}^{NV} f_i^2}} \times 100 \qquad D = \frac{\sqrt{\sum_{i=1}^{NV}(a_i^n - a_i^{n-1})^2}}{\sqrt{\sum_{i=1}^{NV}(a_i^n)^2}} \times 100$$

where NV represents the total number of degrees of freedom. The convergence is achieved when the chosen parameter R or D becomes less than a given tolerance.

5. NUMERICAL EXAMPLES AND DISCUSSION

The validity and suitability of the present unified approach, especially for composite laminated shells, is investigated by considering and evaluating a set of problems. Two computer programs were developed which are based on pseudo-transient analysis: PTFOST5 for predicting linear and geometrically non-linear responses with non-layered approach, and PLPTSHE5 for predicting linear, geometric, material and combined geometric and material non-linear analysis using layered approach. The bi-quadratic nine-noded Lagrangian isoparametric element is employed in the present investigation. The selective integration scheme, namely the 3×3 Gauss quadrature rule, is used to integrate the membrane, coupling between membrane, and bending terms, and a 2×2 Gauss quadrature rule is used to integrate shear energy terms in non-layered approach, whereas in layered approach, either full integration 3×3 or reduced integration 2×2 is adopted for all energy terms. Zero initial conditions are assumed in all the examples of pseudo-transient analysis. All the computations were carried out in single precision on a CDC Cyber 180/840 computer at Indian Institute of Technology, Bombay. Due to bi-axial symmetry of the problems discussed, only one quadrant of shell was analyzed with 2×2 uniform mesh, except angle-ply laminated shells, where the full shell with 4×4 uniform mesh is adopted.

MATERIAL SET 1

The material properties are taken from References [17–19].

$$E_1 = 25 \times E_2$$
$$G_{12} = G_{13} = 0.5 \times E_2$$
$$G_{23} = 0.2 \times E_2$$
$$\nu_{12} = \nu_{23} = \nu_{13} = 0.25$$
$$E_2 = 10^6 \text{ psi}$$

Plasticity parameters

$$\sigma_1^o = 10^4 \text{ psi}$$
$$\sigma_2^o = \sigma_3^o = 4 \times 10^3 \text{ psi}$$
$$\sigma_{12}^o = \sigma_{13}^o = 3.7 \times 10^3 \text{ psi}$$
$$\sigma_{23}^o = 2.3 \times 10^3 \text{ psi}$$

MATERIAL SET 2

The material properties are taken from Reference [20].

$$E_1 = 40 \times E_2$$
$$G_{12} = G_{13} = 0.6 \times E_2$$
$$G_{23} = 0.5 \times E_2$$
$$\nu_{12} = 0.25$$

MATERIAL SET 3

The material properties are taken from Reference [21] (Boran/Epoxy).

$$E_1 = 30 \times 10^6 \text{ psi}$$
$$E_2 = 3.2 \times 10^6 \text{ psi}$$
$$G_{12} = 1.05 \times 10^6 \text{ psi}$$
$$\nu_{12} = 0.21$$
$$G_{23} = G_{13} = G_{12}$$

Plasticity parameters

$$\sigma_1^o = 1.95 \times 10^5 \text{ psi}$$
$$\sigma_2^o = \sigma_3^o = 1.25 \times 10^4 \text{ psi}$$
$$\sigma_{12}^o = 1.8 \times 10^4 \text{ psi}$$
$$\sigma_{13}^o = \sigma_{23}^o = \sigma_{12}^o$$

MATERIAL SET 4

The material properties are taken from Reference [22] (Graphite/Epoxy).

$$E_1 = 18.88 \times 10^6 \text{ psi}$$
$$E_2 = 1.376 \times 10^6 \text{ psi}$$
$$G_{12} = 0.688 \times 10^6 \text{ psi}$$
$$\nu_{12} = 0.343$$
$$G_{23} = G_{13} = G_{12}$$

Plasticity parameters

$$\sigma_1^o = 2.227 \times 10^5 \text{ psi}$$
$$\sigma_2^o = \sigma_3^o = 6.35 \times 10^3 \text{ psi}$$
$$\sigma_{12}^o = 9.92 \times 10^3 \text{ psi}$$
$$\sigma_{13}^o = \sigma_{23}^o = \sigma_{12}^o$$

The finite element displacement formulation developed in this article is based entirely on assumed displacement functions and thus, only displacement boundary conditions are required to be specified. The boundary conditions corresponding to the present formulation are specified in Table 1.

The edge conditions, which have been derived in a variationally consistent manner in the present theory, may not appear so (except in the case of fully clamped edge specified by C), because the natural boundary conditions cannot be prescribed in the displacement based finite element method.

EXAMPLE 1. LINEAR ANALYSIS

Simply supported (S1) symmetric cross-ply (0°/90°/90°/0°) spherical and cylindrical shells with $a/h = 10$, different R/h ratios, and material properties as per material set 1 subjected to a sinusoidal transverse load, are considered. This example is selected to estimate the number of layers in a laminate in the layered approach for accurate results. The results are compared with closed-form and finite element solutions presented by Reddy [18]. Further solutions with parallel formulations based on Sander's shell theory by including shear deformation effects are also repeated. The number of equal thickness layers considered are 4, 8 and 12. The results are presented in Table 2.

A simply supported (S1) unsymmetric cross-ply (0°/90°) spherical shell with $a/h = 100$, different R/a ratios, and the material properties as per material set 1 subjected to uniform transverse load is considered. The present results for 4, 6, 8 and 10 equal thickness layers are compared with Reddy and Liu [19], along with present non-layered approach results. All the formulations are based on Sander's shell theory with constant/first-order shear deformation effects included. The results are presented in Table 3.

From the results of Tables 2 and 3, it is clear that a sufficient number of sub-layers are needed in order to obtain converged results close to non-layered approach results. In pseudo-transient analysis, it is observed that the computer cost of internal force vector computation increases with the increase in the number of sub-layers employed in the through thickness modelling. In the examples considered, 8 to 12 equal thickness sub-layers in a laminate appear to be optimal.

Table 1. Boundary conditions.

Type	$x = 0/x = a$	$x = a/2$	$y = 0/y = b$	$y = b/2$
S1	$v_o = 0 \quad \theta_y = 0$ $w_o = 0$	$u_o = 0 \quad \theta_x = 0$	$u_o = 0 \quad \theta_x = 0$ $w_o = 0$	$v_o = 0 \quad \theta_y = 0$
S2	$u_o = 0 \quad \theta_y = 0$ $w_o = 0$	$u_o = 0 \quad \theta_x = 0$	$v_o = 0 \quad \theta_x = 0$ $w_o = 0$	$v_o = 0 \quad \theta_y = 0$
C	$u_o = 0 \quad v_o = 0$ $\theta_x = 0 \quad \theta_y = 0$ $w_o = 0$	$u_o = 0 \quad \theta_x = 0$	$u_o = 0 \quad v_o = 0$ $\theta_x = 0 \quad \theta_y = 0$ $w_o = 0$	$v_o = 0 \quad \theta_y = 0$

Table 2. Non-dimensional displacement for symmetric laminated cross-ply (0°/90°/90°/0°) shell subjected to sinusoidal transverse load.

Type of Shell	R/h	Reddy [18]		Present Results			
				Non-Layered Approach	Layered Approach		
		CFS	FEM		4	8	12
S	10	0.3223	0.3229	0.3214	0.3288	0.3237	0.3228
	20	0.5254	0.5254	0.5243	0.5477	0.5299	0.5270
	50	0.6362	0.6361	0.6428	0.6756	0.6497	0.6452
	100	0.6559	0.6558	0.6562	0.6984	0.6693	0.6642
	plate	0.6627	0.6627	0.6698	0.7002	0.6729	0.6681
C	10	0.6610	0.6609	0.6661	0.7048	0.6680	0.6634
	100	0.5259	0.5259	0.5677	0.5977	0.5927	0.5694

"S" refers to spherical shell and "C" refers to cylindrical shell.

Table 3. Non-dimensional displacement for an unsymmetric laminated cross-ply (0°/90°) spherical shell subjected to a uniform transverse load.

R/a	Reddy and Liu [19] CFS	Present Results				
		Non-Layered Approach	Layered Approach			
			4	6	8	10
5	0.17535	0.17618	0.18171	0.18028	0.18003	0.17991
10	0.55428	0.55871	0.58691	0.56045	0.56433	0.56170
20	1.12730	1.14067	1.24242	1.16302	1.14134	1.14083
50	1.57140	1.57233	1.78489	1.62302	1.57197	1.57171
100	1.66450	1.66472	1.90507	1.73700	1.66545	1.66430
plate	1.69800	1.69718	1.94444	1.76979	1.70841	1.69425

EXAMPLE 2. GEOMETRICAL NON-LINEAR ANALYSIS (GNL)

A clamped (C) isotropic cylindrical shell with $a = b = 508$ mm, $R = 2540$ mm, $E = 3103$ N/ mm^2 and $\nu = 0.3$ subjected to uniform transverse load, is considered. The present layered approach results with full and uniform reduced integrations are compared with the corresponding present non-layered approach results and other available results in the literature for different a/h ratios (Figure 3). For $a/h = 160$, the displacements obtained with full integration rule are drastically less than those obtained with reduced integration, and non-layered approach with selective integration. This is as expected due to the well-known phenomenon of shear locking in the case of thin shells. Again as expected, shear locking is not visible for $a/h = 100$ and 10. This confirmed that full integration may be employed for $a/h \leq 100$ and reduced integration was necessary for $a/h > 100$ for achieving reasonable accuracy. The following non-dimensional quantities are used in the presentation of results:

$$\hat{q}_o = \frac{q_o}{E_2}\left(\frac{a}{h}\right)^4 \qquad \hat{w}_o = \frac{w_o}{h} \tag{23}$$

Next, a simply supported (SI) nine-layer symmetric cross-ply (0°/90°/ 0°/ . . . /0°) spherical shell with $R/a = 10$, $a/h = 100$, $a = b$, $h = 1$, with material properties as per material set 2 is considered. The present layered approach results are compared with non-layered approach results as well as other

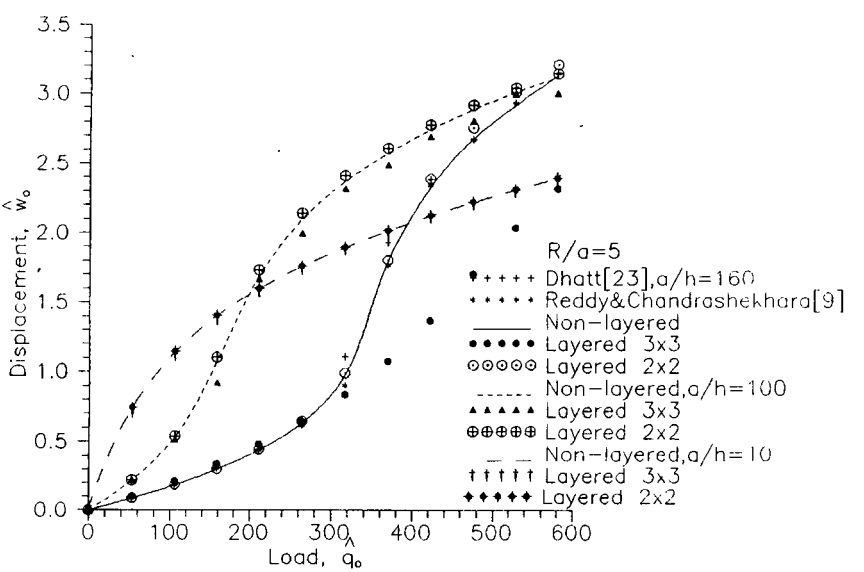

Figure 3. *Displacement vs. load curves for a clamped isotropic cylindrical shell subjected to a uniform transverse load.*

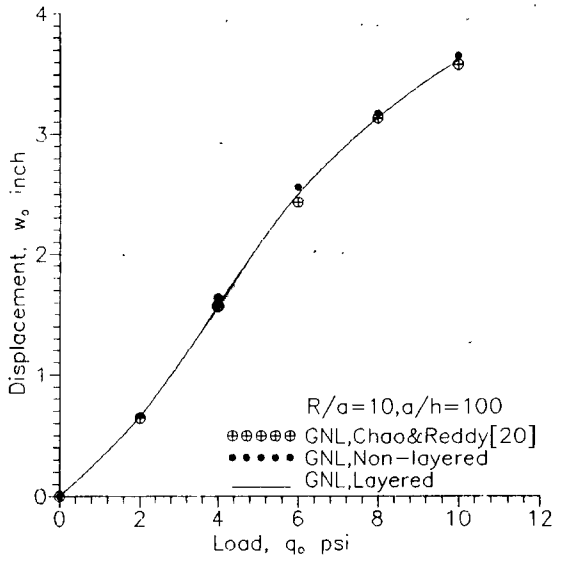

Figure 4. *Displacement vs. load curves for a nine-layered cross-ply (0°/90°/0°/ . . . /0°) spherical shell subjected to a uniform transverse load.*

results of Chao and Reddy [20], and these are plotted in Figure 4. The non-dimensional quantities are as per Equation (23) in these presentations.

Figures 3 and 4 show that all the results are in good agreement. It is to be noted that the shells considered are geometrically thin with negligible shear deformation effects, but this comparison has certainly established the validity of present formulations in the context of geometrically non-linear analysis.

EXAMPLE 3. MATERIALLY NON-LINEAR ANALYSIS (MNL)

A simply supported (S2) cross-ply (0°/90°) spherical shell with $R/a = 10$, $a/h = 100$, $h = 1$ in, and material properties as per material sets 3 and 4 is considered. The laminate is divided into ten equal thickness layers in the layered approach. The present results are compared with those of Reddy and Chandrashekhara [21] and Chandrashekhara [22]. All the computed results and those of others are plotted in Figure 5. Good agreement between present results and other available results, which are based on the Newton-Raphson approach, is evident.

Thus, the present computational model is seen to be reliable in linear, geometrically non-linear, and materially non-linear analyses independently.

EXAMPLE 4. COMBINED NON–LINEAR ANALYSIS (CNL)

To the authors' knowledge, no result is available for combined geometric and material non-linearity. An attempt is made here to study this combined effect.

First, a clamped (C) angle-ply (45°/−45°) spherical shell with $R/a = 10$, $a/h = 10$ and $h = 10$ in, and material properties as per material set 4, is con-

sidered. The laminate is divided into ten equal thickness layers in the layered approach.

The time history of displacement with various approaches is presented in Figure 6, and the results are compared with the corresponding static results which are based on the Newton-Raphson method. The C.P.U. times on CDC Cyber 180/840, in single precision with 16-digit word length accuracy for pseudo-transient linear, geometric non-linear, materially non-linear, and the combined geometric and material non-linear analyses, are 53.4635, 57.7989, 69.1906 and 247.4352 CPU seconds, respectively. The corresponding static Newton-Raphson approach times are 14.9828, 78.8899, 227.4057 and 775.6103 CPU seconds. This clearly shows that there is considerable savings in computational costs, especially in the non-linear analysis with the pseudo-transient method. Hence, the present dynamic relaxation method is a very good alternative to the Newton-Raphson iteration method. The non-dimensional time is defined in these comparisons as

$$\hat{t} = t/\Delta t \tag{24}$$

Secondly, a simply supported (S1) cross-ply (0°/90°/0°) spherical shell with $R/a = 10$, $a/h = 50$ and the material properties given by set 1, is considered. The laminate is divided into nine equal thickness layers. To study the convergence of results, the laminate is divided into 3 × 3 and 4 × 4 uniform meshes in addition to regular 2 × 2 mesh in a quarter laminate. The present results are plotted in Figure 7, with the non-dimensional quantities as per Equation (23).

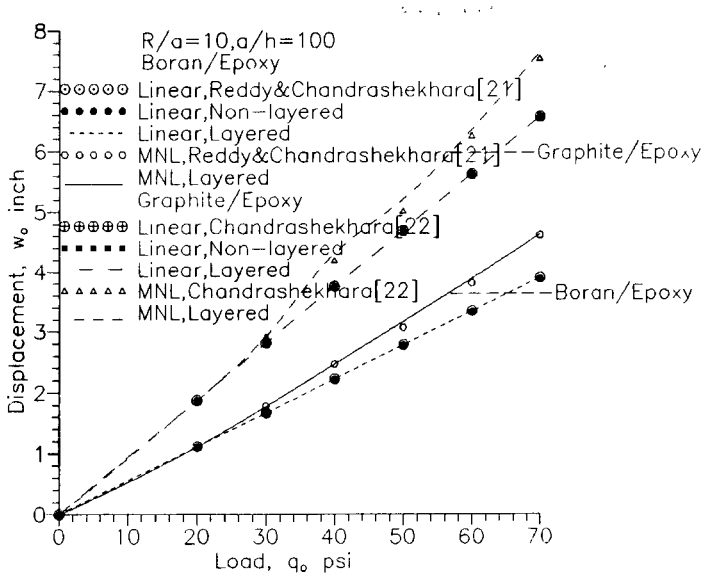

Figure 5. *Dipslacement vs. load curves for a cross-ply (0°/90°) spherical shell subjected to a uniform transverse load.*

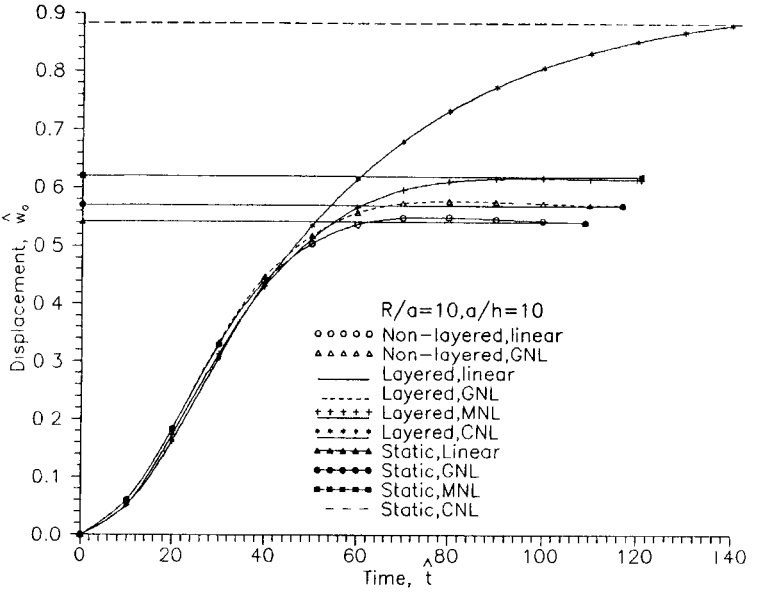

Figure 6. *Time history of displacement for an angle-ply (45°/−45°) spherical shell subjected to a uniform transverse load with adaptive damping.*

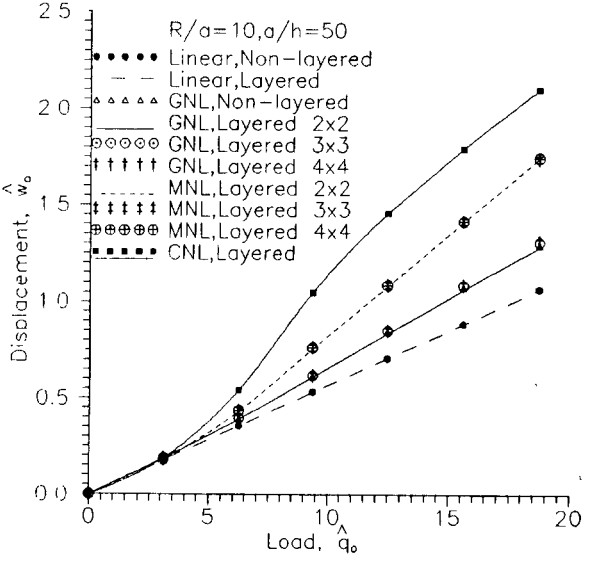

Figure 7. *Displacement vs. load curves for a cross-ply (0°/90°/0°) spherical shell subjected to a uniform transverse load.*

The present layered approach results are compared with the present non-layered approach results in linear as well as geometric non-linear analyses. New results are also presented in material as well as combined geometric and material non-linear analyses. From Figures 6 and 7, it is clear that a 2×2 uniform mesh in a quarter laminate gives the converged results. Further, the combined non-linear response is more than that due to the individual effects, i.e., the shell softens due to the non-linear effects.

6. CONCLUSIONS

The pseudo-transient analysis methodology, based on finite element space discretization, is an adaptation of the dynamic relaxation methodology, which is based on finite difference space discretization and was originally developed in 1965 for solution of both linear and non-linear problems in an unified manner. A comparison of this method with the standard Newton-Raphson method for the solution of the non-linear equations of a problem is not available in literature. An effort in this direction is made here, in the context of large deflection elastostatic/perfectly plastic problems of general fibre reinforced composite shells.

The numerical examples presented in the previous section show a generally good agreement of the present formulation with those from other sources. Thus, this unified approach seems to be capable of solving linear, geometric, material, and combined geometric and material non-linear problems of isotropic/orthotropic and anisotropic material properties. It is important to note that the computer code developed here requires very small core memory as compared to other static programs. It is further noted that this method will give solutions of very large linear and non-linear finite element problems on small computers. Another important merit of the present unified approach is its easy implementation. The only computational effort involved is in the computation of internal force vector **P**, in which any extent of non-linearity can be easily included.

ACKNOWLEDGEMENT

Partial support of this research by the Aeronautics Research and Development Board, Ministry of Defense, Government of India through its Grant Nos. Aero/RD-134/100/10/88-89/518 and Aero/RD-134/100/10/88-89/534 is greatly acknowledged.

APPENDIX A

Flow Theory of Plasticity

Yield criterion: For the anisotropic materials to be considered in this work, the yield criterion employed will be a generalization of the Huber-Mises law. The yield criterion can be written in the general form as (see Hinton and Owen [25])

$$F(\sigma,\psi) = f(\sigma) - y(\psi) = 0 \tag{A1}$$

in which f is some function of the deviatric stress invariants, and the yield level y can be a function of hardening parameter, ψ.

Defining the plastic potential, or effective stress, σ_{ef}, in a similar manner to the Huber-Mises yield function for isotropic materials, it can be written as,

$$f = \sigma_{ef}^2 = [\alpha_{12}(\sigma_1 - \sigma_2)^2 + \alpha_{23}(\sigma_2 - \sigma_3)^2 + \alpha_{13}(\sigma_3 - \sigma_1)^2 + 3\alpha_{44}\tau_{12}^2 + 3\alpha_{55}\tau_{13}^2 + 3\alpha_{66}\tau_{23}^2] \tag{A2a}$$

where σs (τs) are stress components, the αs are parameters of anisotropy, and the subscripts 1, 2, 3 refer to the direction of three principal axes of anisotropy. Developing this expression by assuming $\sigma_3 = \sigma_z = 0$, the effective stress can be written as,

$$\sigma_{ef}^2 = a_{11}\sigma_1^2 + 2a_{12}\sigma_1\sigma_2 + a_{22}\sigma_2^2 + a_{33}\tau_{12}^2 + a_{44}\tau_{13}^2 + a_{55}\tau_{23}^2 \tag{A2b}$$

where a_{11}, a_{12}, a_{22}, a_{33}, a_{44} and a_{55} are anisotropic parameters which can be determined experimentally.

If the principal axes of anisotropy 1,2 do not coincide with the reference axes x, y but are rotated by a certain angle θ, then the anisotropic parameters for the new system are changed according to the stress transformation. In matrix form, Equation (A2b) can be written as,

$$\sigma_{ef}^2 = \boldsymbol{\sigma}_{1,2,3}\bar{\mathbf{A}}\boldsymbol{\sigma}_{1,2,3} \tag{A3a}$$

where

$$\bar{\mathbf{A}} = \begin{bmatrix} \bar{a}_{11} & \bar{a}_{12} & 0 & 0 & 0 \\ \bar{a}_{12} & \bar{a}_{22} & 0 & 0 & 0 \\ & & \bar{a}_{33} & 0 & 0 \\ \text{symmetric} & & & \bar{a}_{44} & 0 \\ & & & & \bar{a}_{55} \end{bmatrix} \tag{A3b}$$

The equation of stress transformation is

$$\boldsymbol{\sigma}_{1,2,3} = \mathbf{T}\boldsymbol{\sigma}_{x,y,z} \tag{A4}$$

where $\mathbf{T}$ is the transformation matrix. The effective stress, expressed in reference system x, y and z, is then

$$\sigma_{ef}^2 = \boldsymbol{\sigma}_{x,y,z}^t\bar{\mathbf{A}}\boldsymbol{\sigma}_{x,y,z} \tag{A5a}$$

in which $\bar{\mathbf{A}}$ is the matrix of the new anisotropic parameters given by

$$\bar{\mathbf{A}} = \begin{bmatrix} a_{11} & a_{12} & a_{13} & 0 & 0 \\ a_{12} & a_{22} & a_{23} & 0 & 0 \\ & & a_{33} & 0 & 0 \\ \text{symmetric} & & & \bar{a}_{44} & a_{45} \\ & & & & \bar{a}_{55} \end{bmatrix} \tag{A5b}$$

The coefficients of the matrix **A** corresponding to the L^{th} layer are defined as follows

$$
\begin{aligned}
a_{11} &= \bar{a}_{11} \cdot c^4 + (2\bar{a}_{12} + \bar{a}_{33}) \cdot s^2 \cdot c^2 + \bar{a}_{22} \cdot s^4 \\
a_{12} &= \bar{a}_{12} \cdot (c^4 + s^4) + (\bar{a}_{11} + \bar{a}_{22} - \bar{a}_{33}) \cdot s^2 \cdot c^2 \\
a_{13} &= (2\bar{a}_{11} - 2\bar{a}_{12} - \bar{a}_{33}) \cdot s \cdot c^3 + (2\bar{a}_{12} - 2\bar{a}_{22} + \bar{a}_{33}) \cdot s^3 \cdot c \\
a_{22} &= \bar{a}_{11} \cdot s^4 + (2\bar{a}_{12} + \bar{a}_{33}) \cdot s^2 \cdot c^2 + \bar{a}_{22} \cdot c^4 \\
a_{23} &= (2\bar{a}_{11} - 2\bar{a}_{12} - \bar{a}_{33}) \cdot s^3 \cdot c + (2\bar{a}_{12} - 2\bar{a}_{22} + \bar{a}_{33}) \cdot s \cdot c^3 \\
a_{33} &= \bar{a}_{33} \cdot (c^4 + s^4) + (4\bar{a}_{11} - 8\bar{a}_{12} + 4\bar{a}_{22} - 2\bar{a}_{33}) \cdot s^2 \cdot c^2 \\
a_{44} &= \bar{a}_{44} \cdot c^2 + \bar{a}_{55} \cdot s^2 \\
a_{45} &= (\bar{a}_{44} - \bar{a}_{55}) \cdot c \cdot s \\
a_{55} &= \bar{a}_{44} \cdot s^2 + \bar{a}_{55} \cdot c^2
\end{aligned}
\tag{A5c}
$$

The parameters of anisotropy can be determined by six independent yield tests. The initial parameters (no hardening effects) are obtained by successively allowing all stress components to be zero in the yield function Equation (A5a), except the one under consideration. For a tensile test in the 1 direction,

$$a_{10} = \sigma_{oef}^2 / \sigma_{10}^2 \tag{A6a}$$

where σ_{oef} is the uniaxial yield stress in the reference direction, and σ_{10} is the uniaxial yield stress in the 1 direction. Taking the 1 direction as the reference direction, $a_{10} = 1.0$.

Similarly,

$$
\begin{aligned}
a_{20} &= \sigma_{oef}^2 / \sigma_{10}^2 \\
a_{30} &= \sigma_{oef}^2 / \tau_{120}^2 \\
a_{40} &= \sigma_{oef}^2 / \tau_{130}^2 \\
a_{50} &= \sigma_{oef}^2 / \tau_{230}^2
\end{aligned}
\tag{A6b}
$$

To obtain a_{120}, another uniaxial tensile test is required in which the specimen

is taken from the $\overline{12}$ material surface. If the specimen axis is rotated by an angle ϕ to the 1 axis, and assuming $\sigma_{\phi o}$ as the uniaxial stress obtained by test, then

$$\begin{aligned} \sigma_1 &= \sigma_{\phi o} \cos^2 \phi \\ \sigma_2 &= \sigma_{\phi o} \sin^2 \phi \\ \tau_{12} &= \sigma_{\phi o} \cos \phi \sin \phi \\ \tau_{13} &= \tau_{23} = 0 \end{aligned} \tag{A7a}$$

Substituting these stress components in Equation (A4a) and assuming $\phi = 45°$, the remaining parameter can be obtained as,

$$a_{12} = 2(\sigma_{oef}/\sigma_{\phi o})^2 - \frac{1}{2}(1.0 + a_{20} + a_{30}) \tag{A7b}$$

These parameters are functions of the current yield stress; therefore, they must vary for a work-hardening material. Their subsequent values are obtained by introducing the current yield stress values into Equations (A1a) to (A7b). However, in the present investigations, the work-hardening effects are not included.

The flow vector is now defined as,

$$\mathbf{a} = \begin{bmatrix} \dfrac{\partial \sigma_{ef}}{\partial \sigma_x} \text{(a1)} \\ \dfrac{\partial \sigma_{ef}}{\partial \sigma_y} \text{(a2)} \\ \dfrac{\partial \sigma_{ef}}{\partial \tau_{xy}} \text{(a3)} \\ \dfrac{\partial \sigma_{ef}}{\partial \tau_{xz}} \text{(a4)} \\ \dfrac{\partial \sigma_{ef}}{\partial \tau_{yz}} \text{(a5)} \end{bmatrix}^L = \frac{1}{\sqrt{\sigma_{ef}}} \begin{bmatrix} a_{11}\sigma_x + a_{12}\sigma_y + a_{13}\tau_{xy} \\ a_{12}\sigma_x + a_{22}\sigma_y + a_{23}\tau_{xy} \\ a_{13}\sigma_x + a_{23}\sigma_y + a_{33}\tau_{xy} \\ a_{44}\tau_{xz} + a_{45}\tau_{yz} \\ a_{45}\tau_{xz} + a_{55}\tau_{yz} \end{bmatrix}^L \tag{A8}$$

REFERENCES

1. Day, A. S. 1965. "An Introduction to Dynamic Relaxation," *Engr. Lond.*, pp. 219–221.
2. Rushton, K. R. 1968. "Dynamic Relaxation Solution of Elastic Problems," *J. Strain Anal.*, 3:24–32.
3. Rushton, K. R. 1969. "Dynamic Relaxation Solution for Large Deflection of Plates with Specified Boundary Stresses," *J. Strain Anal.*, 4:75–80.

4. Brew, J. S. and D. M. Brotton. 1971. "Non-Linear Structural Analysis by Dynamic Relaxation," *Int. J. Numer. Meth. Engng.*, 3:463–483.
5. Alwar, R. S. and N. Ramachandra Rao. 1974. "Large Elastic Deformation of Clamped Skew Plates by Dynamic Relaxation," *Comput. Struct.*, 4:381–398.
6. Pica, A. and E. Hinton. 1980. "Transient and Pseudo-Transient Analysis of Mindlin Plates," *Int. J. Numer. Meth. Engng.*, 15:189–208.
7. Pica. A. and E. Hinton. 1981. "Further Developments in Transient and Pseudo-Transient Analysis of Mindlin Plates," *Int. J. Numer. Meth. Engng.*, 17:1749–1761.
8. Kant, T. and S. Patel. 1990. "Transient/Pseudo-Transient Finite Element Small/Large Deformation Analysis of Two Dimensional Problems," *Comput. Struct.*, 36:421–427.
9. Reddy, J. N. and K. Chandrashekhara. 1985. "Non-Linear Analysis of Laminated Shells Including Transverse Shear Strains," *AIAA J.*, 23:440–441.
10. Sanders, J. L. 1959. "An Improved First Approximation Theory for Thin Shells," NASA TR, p. 24.
11. Kant, T. and J. R. Kommineni. 1992. "Geometrically Non-Linear Analysis of Doubly Curved Laminated and Sandwich Fibre Reinforced Composite Shells with a Higher Order Theory and C° Finite Elements," *J. Reinforced Plastics and Composites*, 11:1048–1076.
12. Owen, D. R. J. and E. Hinton. 1980. *Finite Elements in Plasticity.* West Cross, Swansea, U. K.: Pineridge Press Limited, p. 91.
13. Zienkiewicz, O. C. 1977. *The Finite Element Method, Third Edition.* London: McGraw-Hill.
14. Reddy, J. N. 1985. *An Introduction to the Finite Element Method.* New York, NY: McGraw-Hill.
15. Rushton, K. R. and L. M. Laing. 1968. "A Digital Computer Solution of the Laplace Equation Using the Dynamic Relaxation Method," *Aeronautic. Quart.*, 19:375–387.
16. Rushton, K. R. "Large Deflection of Variable Thickness Plates," *Int. J. Mech. Sci.*, 10:723–735.
17. Nanda, A. and T. Kuppusamy. 1991. "Three Dimensional Elastic-Plastic Analysis of Laminated Composite Plates," *Composite Struct.*, 17:213–225.
18. Reddy, J. N. 1982. "Bending of Laminated Anisotropic Shells by a Shear Deformable Finite Element," *Fibre Sci. Tech.*, 17:2–24.
19. Reddy, J. N. and C. F. Liu. 1985. "A Higher Order Shear Deformation Theory of Laminated Elastic Shells," *Int. J. Engng. Sci.*, 23:319–330.
20. Chao, W. C. and J. N. Reddy. 1983. "Geometrically Non-Linear Analysis of Layered Composite Shells," in *Mechanics of Composite Materials, AMD*, G. J. Dvorak, ed., New York, NY: ASME Publication, 58:19–31.
21. Reddy, J. N. and K. Chandrashekhara. 1985. "Non-Linear Finite Element Models of Laminated Plates and Shells," in *Finite Elements in Computational Mechanics*, T. Kant, ed., London, Pergamon Press, 1:189–209.
22. Chandrashekhara, K. "General Non-Linear Bending Analysis of Composite Beams, Plates and Shells," in *Composite Materials and Structures, Proc. Int. Conf.*, K. V. A. Pandalai and S. K. Malhotra, eds., New Delhi, India: Indian Institute of Technology, Madras, Tata McGraw-Hill Publishing Co., pp. 392–402.
23. Dhatt, G. S. 1970. "In-Stability of Thin Shells by Finite Element Method," in *IASS Symposium for Folded Plates and Prismatic Structures, Vienna.*
24. Kant, T. and J. R. Kommineni. In press. "Pseudo-Transient Large Deflection Elastic Analysis of Fibre Reinforced Composite Plates," *Int. J. Engineering Computations.*
25. Hinton, E. and D. R. J. Owen. 1984. *Finite Element Software for Plates and Shells.* Swansea, U.K.: Pineridge Press Limited.